HHS Public Access

Author manuscript

J Cardiovasc Transl Res. Author manuscript; available in PMC 2023 February 01.

Published in final edited form as:

J Cardiovasc Transl Res. 2022 February ; 15(1): 15–26. doi:10.1007/s12265-021-10155-3.

Renal Revascularization Attenuates Myocardial Mitochondrial Damage and Improves Diastolic Function in Pigs with Metabolic Syndrome and Renovascular Hypertension

Rahele A. Farahani[1], **Shasha Yu**[1], **Christopher M. Ferguson**[1], **Xiang-Yang Zhu**[1], **Hui Tang**[1], **Kyra L. Jordan**[1], **Ishran M. Saadiq**[1], **Sandra M. Herrmann**[1], **Alejandro R. Chade**[2], **Amir Lerman**[3], **Lilach O. Lerman**[1,3], **Alfonso Eirin**[1]

[1]Division of Nephrology and Hypertension, Department of Internal Medicine, Mayo Clinic, 200 First Street SW, Rochester, MN, 55905, USA

[2]Department of Physiology and Biophysics, University of Mississippi Medical Center, Jackson, MS, USA

[3]Department of Cardiovascular Diseases, Mayo Clinic, Rochester, MN, USA

Abstract

Percutaneous transluminal renal angioplasty (PTRA) may improve cardiac function in renovascular hypertension (RVH), but its effect on the biological mechanisms implicated in cardiac damage remains unknown. We hypothesized that restoration of kidney function by PTRA ameliorates myocardial mitochondrial damage and preserves cardiac function in pigs with metabolic syndrome (MetS) and RVH. Pigs were studied after 16 weeks of MetS+RVH, MetS+RVH treated 4 weeks earlier with PTRA, and Lean and MetS Sham controls (n=6 each). Cardiac function was assessed by multi-detector CT, whereas cardiac mitochondrial morphology and function, microvascular remodeling, and injury pathways were assessed ex vivo. PTRA attenuated myocardial mitochondrial damage, improved capillary and microvascular maturity, and ameliorated oxidative stress and fibrosis, in association with attenuation of left ventricular remodeling and diastolic dysfunction. Myocardial mitochondrial damage correlated with myocardial injury and renal dysfunction. Preservation of myocardial mitochondria with PTRA can enhance cardiac recovery, underscoring its therapeutic potential in experimental MetS+RVH.

eirinmassat.alfonso@mayo.edu .

Ethics Approval

This article does not contain any studies with human participants. All animal studies were approved by the Mayo Clinic Animal Care and Use Committee.

Conflict of Interest

The authors declare no competing interests.

Keywords

Renovascular hypertension; Cardiac dysfunction; Metabolic syndrome; Mitochondria; Revascularization

1. Introduction

Renovascular hypertension (RVH), defined as high blood pressure caused by partial or complete occlusion of one or both renal arteries, accelerates tissue injury in the post-stenotic kidney and may lead to end-stage renal disease [1]. Importantly, RVH imposes a greater risk of cardiovascular complications and may lead to abnormalities in cardiac structure and function [2]. Patients with RVH often manifest with metabolic syndrome (MetS), which fosters an increased risk for heart failure [3], increasing cardiovascular morbidity and mortality.

Percutaneous transluminal renal angioplasty (PTRA) is a procedure that restores renal artery patency and blood flow beyond a stenotic lesion. In patients with RVH, renal artery revascularization has been shown to improve cardiac function and reduce hear failure hospitalizations [4]. Yet, uncertainty remains regarding the effect of PTRA on the primary biological mechanisms implicated in cardiac damage in RVH.

Mitochondria are cardiomyocyte powerhouses that produce adenosine triphosphate (ATP) through oxidative phosphorylation to sustain the high-energy demand of the heart. Cardiac mitochondria are arranged in packed strands located between the myofibrils (interfibrillar mitochondria) or situated underneath the sarcolemmal membrane (subsarcolemmal mitochondria) [5]. In addition to produce energy, these organelles regulate other important cellular process, such as generation of reactive oxygen species (ROS), cellular proliferation, calcium signaling, and apoptosis [6]. We have previously shown that early MetS in swine induces cardiomyocyte mitochondrial disorganization, associated with myocardial vascular impairment, oxidative stress, and apoptosis [7, 8]. Likewise, RVH in swine induces important mitochondrial structural abnormalities and dysfunction, associated with cardiac remodeling and impaired left ventricular (LV) relaxation [9], whereas the combination of MetS and RVH in swine is associated with myocardial mitochondrial morphological abnormalities, increased production of ROS, and impaired energy production [10].

Our recent study in a well-established swine model of coexisting MetS and RVH [11–13] has shown that PTRA attenuates renal mitochondrial injury and preserves post-stenotic kidney function without affecting systemic hypertension [14]. However, the potential of PTRA to ameliorate myocardial mitochondrial damage and preserve cardiac structure and function despite sustained RVH remains unclear. This study tested the hypothesis that restoration of ischemic kidney function by PTRA attenuates myocardial mitochondrial damage and preserves cardiac structure and function in swine MetS+RVH.

2. Materials and Methods

All animal studies were approved by our Institutional Animal Care and Use Committee. We studied 24 female domestic pigs after 16 weeks of observation (Figure S1). At baseline pigs were randomized into two groups: Lean group (n=6) and MetS group (n=18). Lean pigs were fed standard pig chow, whereas MetS pigs were fed a high-cholesterol/high-carbohydrate diet consisting of 17% protein, 20% complex carbohydrates, 20% fructose, and 43% fat, supplemented with 2% cholesterol and 0.7% sodium cholate by weight [15] for the duration of the study. We have shown that pigs fed with a MetS diet for 12–16 weeks developed progressive increases in blood pressure and MetS [15].

Six weeks later, all Lean and MetS pigs were anesthetized with 0.25g of IM tiletamine hydrochloride/zolazepam hydrochloride (Telazol®, Fort Dodge Animal Health, New York) and 0.5g of xylazine, and anesthesia maintained with 0.2mg/kg/min of IV ketamine and 0.03mg/kg/min of IV xylazine. RVH was induced in 12 MetS pigs by placing an irritant coil in the main renal artery using fluoroscopy, as previously described [16], whereas a Sham procedure was performed in the remaining 6 MetS and 6 Lean pigs. We have previously shown that placing an irritant coil in the main renal artery leads to development of hypertension within 1–2 weeks [17–20].

Six weeks after the induction of RVH or Sham, all animals were similarly anesthetized, and the degree of stenosis was determined by angiography. PTRA was performed in 6 RVH pigs, as previously described [18]. Under fluoroscopic guidance, a balloon catheter with a mounted tantalum stent was engaged in the proximal-middle section of the renal artery and inflated to a high pressure. This resulted in expansion of the stent to full balloon diameter and restoration of the luminal opening. The balloon was kept inflated for 5–10 min and then deflated and removed, leaving the stent embedded in the vascular wall. Technical success was judged by repeating angiography 10–15 min (and 4 weeks) later. Lean, MetS, and the remaining MetS+RVH pigs underwent a Sham procedure.

Four weeks after PTRA or Sham, all pigs were again similarly anesthetized and systemic blood samples collected to measure plasma renin activity (PRA, GammaCoat kit; DiaSorin), serum creatinine (spectrophotometry) [21], monocyte chemoattractant protein (MCP)-1, interleukin (IL)-6 (ELISA), 8-isoprostane (enzyme immunoassay kit), and N-terminal pro-brain natriuretic peptide (NT-proBNP, ELISA, Abclonal Cat#: RK03083) levels. Cardiac function was assessed using multi-detector computed tomography (MDCT), and blood pressure was measured with an intra-arterial catheter during MDCT studies.

Three days after completion of MDCT studies, pigs were euthanized with an i.v. bolus of 100mg/kg of sodium pentobarbital (Fatal-Plus, Vortech Pharmaceuticals, Dearborn). Hearts were harvested and LV tissue sections frozen in liquid nitrogen (and maintained at −80°C) or preserved in formalin or Trump’s fixative for ex vivo studies. In addition, a segment of the LV was prepared for micro-CT studies.

2.1. In Vivo Studies

2.1.1. Cardiac and Renal Function—Cardiac function was assessed using an MDCT scanner (Somatom Sensation-128, Siemens Medical Solution, Forchheim, Germany) [22]. The entire LV was scanned 20 times throughout the cardiac cycle to measure ejection fraction, whereas LV endocardial and epicardial borders were traced to calculate LV muscle mass (LVMM) [23]. Images were analyzed with the Analyze™ software package (Biomedical Imaging Resource, Mayo Clinic, MN). Early (E) and late (A) ventricular filling rates were calculated from the positive slopes of volume/time curves and E/A ratio calculated using MATLAB® (Math-Work, Natick, MA, USA) [24]. The left atrium (LA) was traced at end-diastole for volumetric quantification. Single-kidney volume, renal blood flow (RBF), and glomerular filtration rate (GFR) were determined using an MDCT scanner (Flash 128 MDCT scanner, Somatom Definition Flash, Siemens Healthcare) [20, 25]. Scans were performed following a bolus of iopamidol (0.5cc/kg over 2 s). Single-kidney volume, RBF, and GFR were calculated, as previously described (Analyze, Biomedical Imaging Resource, Mayo Clinic, Rochester, MN) [26, 27].

2.2. Ex Vivo Studies

2.2.1. Cardiac Mitochondrial Structure—We assessed myocardial mitochondrial morphology using a transmission electron microscope (Philips CM10). LV samples (2–3mm^3) were fixed with Trump's fixative (4% formaldehyde and 0.1% glutaraldehyde in 0.1M phosphate buffer) overnight at room temperature, mounted on mesh grids, stained with aqueous uranyl acetate and lead citrate, and processed at the Mayo Clinic's electron microscopy core facility. For analysis, 10 representative cardiomyocytes were randomly selected, and only mitochondria fully contained within the borders of the transmission electron microscopy images were analyzed [7]. Interfibrillar, subsarcolemmal, and endothelial cell mitochondrial density (number of mitochondria/field), area (nm^2), and matrix density (1/mean gray values in arbitrary units) were determined using the "freehand tool" of the National Institutes of Health software ImageJ (version 1.5).

2.2.2. Cardiac Mitochondrial Function—Mitochondrial oxidative stress and bioenergetics were assessed in isolated cardiac mitochondria (MITO-ISO kit, Catalog #8268, ScienCell, Carlsbad, California), as previously shown [28]. Frozen LV tissue (10mg) was resuspended in 10μl of assay buffer and homogenized (10–15 passes). Samples were subsequently centrifuged (microcentrifuge 13226g for 5min), and the supernatant was collected and deproteinized. Deproteinized samples (50μl) were then added into a plate and read (OD570nm). Mitochondrial hydrogen peroxide (H_2O_2) production was measured by colorimetric quantitative methods (OxisResearch, BIOXYTECH® H2O2-560™ Assay, Cat# 21024) [28], whereas ATP generation (ATP/ADP ratio) and cytochrome-c oxidase (COX-IV) activity (absorbance units/mg protein) were assessed by colorimetric and fluorometric methods (Abcam Cat# ab83355 and Abnova Cat# KA3950, respectively).

2.2.3. Cardiac Injury—Myocardial in situ production of superoxide anion was detected by dihydroethidium (DHE) staining (20μM/l; Sigma) [7], and myocardial capillary density was determined by CD31 staining (Bio-Rad, Oxford, UK). In addition, myocyte cross-sectional area and myocardial fibrosis were calculated in wheat germ agglutinin (WGA)-

and trichrome-stained slides, respectively. All staining images were semi-automatically quantified in 15–20 fields and the results from all fields averaged [29]. Myocardial microvascular structure was assessed by micro-CT, as previously described [24]. The LV wall was perfused under physiological pressure with an intravascular contrast agent (MV-122; Flow Tech, Carver, MA) through a branch of the left circumflex coronary artery. A transmural portion (2 cm^3) of the LV was scanned, and images were analyzed with Analyze™. Spatial density of microvessels (20-500μm) in the subepicardium and subendocardium and vessel tortuosity (an index of vessel immaturity) were calculated, as previously described [24].

2.3. Statistical Analysis

JMP Pro version 14 (SAS) software was used to perform all statistical analyses. Results were expressed as mean ± SD. Comparison between and among the groups was performed using parametric (ANOVA and 2-tailed Student's *t*-test) and nonparametric (Wilcoxon and Kruskal-Wallis) methods when appropriate. Regressions were calculated by the least-squares fit to compare myocardial mitochondrial damage and cardiac injury after PTRA. p values<0.05 were considered statistically significant.

3. Results

Six weeks after induction of RVH and immediately before PTRA, all MetS+RVH pigs developed hemodynamically significant stenosis (79.6%±3.6% vs. 72.5%±5.4%, p=0.30 ANOVA), and their blood pressure was similarly elevated (p<0.05 vs. Lean+Sham in all).

Table 1 summarizes the baseline characteristics and cardiac function of Lean+Sham, MetS+Sham, MetS+RVH, and MetS+RVH+PTRA groups at 16 weeks and 4 weeks after PTRA or Sham. Body weight was equally higher in MetS+Sham, MetS+RVH, and MetS+RVH+PTRA compared to Lean+Sham. The degree of stenosis was higher in MetS+RVH compared to Sham groups, but PTRA completely restored renal artery patency. Heart rate did not differ among the groups, whereas systolic, diastolic, and mean arterial pressure were similarly elevated in MetS+Sham and MetS+RVH groups compared to Lean+Sham and remained elevated in MetS+RVH+PTRA. Single-kidney volume, RBF, and GFR were higher in MetS compared to Lean pigs, decreased in MetS+RAS, but increased in PTRA-treated pigs, whereas PRA levels were similar among the groups. Circulating MCP-1 and IL-6 levels were higher in MetS+RVH compared to Lean+Sham and MetS+Sham but decreased in PTRA-treated pigs. Contrarily, circulating isoprostane levels were higher in MetS+Sham compared to Lean+Sham and further and similarly increased in MetS+RVH and MetS+RVH+PTRA groups. Contrarily, serum creatinine levels were higher in MetS+RVH compared to Sham groups but decreased in MetS+RVH+PTRA, as did LA end-diastolic volume (EDV), and LVMM. Ejection fraction was similar among the groups, whereas E/A (early and late ventricular filling) ratio that decreased in MetS+RVH versus Lean+Sham and MetS+Sham groups increased in MetS+RVH+PTRA pigs. Circulating NT-proBNP levels were higher in MetS+RVH compared to Lean+Sham and MetS+Sham but decreased in PTRA-treated pigs.

3.1. PTRA Attenuated Myocardial Mitochondrial Structural Damage

Interfibrillar mitochondrial density was similar among the groups (Figure 1), but mitochondrial area was higher and matrix density lower in MetS+RVH compared to Lean+Sham and MetS+Sham groups. Yet, treatment with PTRA decreased interfibrillar mitochondrial area and increased matrix density. Subsarcolemmal mitochondrial density that decreased in MetS+Sham compared to Lean+Sham further decreased in MetS+RVH, but slightly improved in MetS+RVH+PTRA (Figure S2). Contrarily, subsarcolemmal mitochondrial area and matrix density were similar among the groups. Cardiac endothelial cell mitochondrial density that decreased in MetS+Sham and further decreased in MetS+RVH increased to MetS+Sham levels in PTRA-treated pigs (Figure S3). Although endothelial cell mitochondrial area did not differ among the groups, matrix density that decreased in MetS+RVH compared to Sham was restored in MetS+RVH+PTRA pigs.

3.2. PTRA Improved Cardiac Mitochondrial Function

Production of H_20_2 in isolated cardiac mitochondria was higher in MetS+Sham versus Lean+Sham and further increased in MetS+RVH but was restored to Lean+Sham levels in MetS+RVH+PTRA-treated pigs (Figure 2A). Mitochondrial COX-IV activity and ATP generation that decreased in MetS+Sham compared to Lean+Sham and further decreased in MetS+RVH improved in PTRA-treated pigs (Figure 2B).

3.3. PTRA Ameliorated Cardiac Injury

Myocardial superoxide production increased in MetS+Sham compared to Lean+Sham, further increased in MetS+RVH, but decreased in MetS+RVH+PTRA pigs (Figure 3). Myocardial capillary density (CD31+ staining) that slightly decreased in MetS+Sham and further decreased in MetS+RVH improved in MetS+RVH+PTRA pigs. Spatial density of larger subepicardial microvessels as determined by micro-CT was comparable between Lean+Sham and MetS+Sham pigs but similarly decreased in RVH groups (Figure 4A–B). However, vessel tortuosity that increased in MetS+Sham compared to Lean+Sham and further increased in MetS+RVH decreased in MetS+RVH+PTRA pigs, suggesting improvement of vessel maturity (Figure 4A–C). Myocyte cross-sectional area was higher in MetS+RVH versus Sham groups but was restored in MetS+RVH+PTRA pigs, whereas myocardial fibrosis that increased in MetS+Sham compared to Lean+Sham and further increased in MetS+RVH decreased in PTRA-treated pigs (Figure 5).

3.4. Cardiac Mitochondrial Damage Correlated with Myocardial Injury

Myocardial mitochondrial matrix density correlated inversely with myocardial fibrosis (Figure 6A), whereas endothelial cell mitochondrial density correlated directly with myocardial capillary density (Figure 6B). A direct correlation was also found between subsarcolemmal mitochondrial density and mitochondrial ATP generation (Figure 6C). Moreover, mitochondrial production of H_20_2 correlated directly with myocardial superoxide generation (Figure 6D). Myocardial mitochondrial matrix density and ATP generation correlated directly with stenotic kidney GFR (Figure 6E–F).

4. Discussion

The current study shows that despite sustained RVH, improvement of ischemic kidney function by PTRA ameliorated myocardial mitochondrial damage and diastolic dysfunction in pigs with coexisting MetS and RVH. We found that 4 weeks after technically successful renal revascularization, cardiomyocyte mitochondrial structure and function, which were impaired in MetS+RVH pigs, improved in PTRA-treated pigs, associated with attenuation of myocardial oxidative stress, and improved capillary density and microvascular maturity. PTRA also attenuated MetS+RVH-induced LV remodeling and fibrosis and improved diastolic function. Importantly, myocardial mitochondrial damage correlated with stenotic kidney GFR, suggesting that improvement of renal function might be an important mechanism by which PTRA preserves myocardial mitochondria and attenuates cardiac injury in experimental MetS+RVH.

RVH is a common cause of heart failure strongly associated with increased cardiovascular morbidity and mortality [30]. A cross-sectional study of 79 patients with RVH revealed that they exhibit a high prevalence of cardiac morphologic and functional abnormalities, such as LV hypertrophy and diastolic dysfunction, and only 5% of them had normal cardiac structure and function [31]. Although PTRA does not confer additional benefit over conventional medical therapy with respect to prevention of clinical cardiovascular events [32], prospective studies suggest that restoration of renal artery patency may have important clinical and potential mortality benefits in high-risk patients [33]. Similarly, Kane and colleagues studied patients with RVH and heart failure and found that renal revascularization was associated with a significant decrease in the New York Heart Association Functional Class and a 5-fold reduction in the number of hospitalizations [4], underscoring the therapeutic potential of PTRA to preserve cardiac structure and function in patients with RVH.

In this study, we investigated the effect of PTRA on myocardial mitochondria, which maintain cellular respiration and modulate several important cellular functions, such as generation of reactive oxygen species [6]. Our previous studies in swine models of MetS [7, 8] and RVH [9] revealed that cardiomyocyte mitochondria exhibit important structural abnormalities and dysfunction, associated with cardiac remodeling and impaired LV relaxation [9]. More recently, we have shown in swine MetS+RVH that PTRA attenuates renal mitochondrial injury and preserves post-stenotic kidney function without affecting systemic hypertension [14]. This study extends our previous observations and demonstrates that despite similar blood pressure levels, PTRA also protects myocardial mitochondrial structure, disclosed by decreased interfibrillar mitochondrial swelling (increased mitochondrial area) and cristae remodeling (decreased matrix density). In addition, PTRA increased the number of subsarcolemmal mitochondria, which are tightly joined beneath the cardiomyocyte plasma membrane to provide energy for electrolyte and protein transport across the sarcolemma [34]. This suggests increased deficiency for energy production and is consistent with our observation that subsarcolemmal mitochondrial density correlated directly with cardiac mitochondrial ATP generation.

Preservation of cardiomyocyte mitochondrial structure could have potentially attenuated electron leakage and ROS production and sustained energy production. Indeed, the rate of generation of H_2O_2, produced by leaks of electrons from donor redox centers of the mitochondrial electron transport chain [35], decreased in MetS+RVH+PTRA pigs. Furthermore, PTRA increased the activity of COX-IV, a major regulation site for oxidative phosphorylation [36], as did generation of ATP. Excessive production of H_20_2 damages mitochondrial proteins, lipids, and DNA and compromises ATP synthesis [37]. Therefore, attenuation of mitochondrial ROS production by PTRA could have contributed to preserve cardiomyocyte mitochondrial structure and bioenergetics.

Interestingly, we found that PTRA increased endothelial cell mitochondrial number and matrix density. Although the number of mitochondria is significantly lower in endothelial cells compared to cardiomyocytes, these organelles modulate several important factors that regulate vascular function [38]. We have previously shown that diet-induced MetS in swine decreased coronary endothelial cell mitochondrial density, associated with vascular remodeling and dysfunction [8]. Likewise, RVH in swine decreased the content of the mitochondrial phospholipid cardiolipin, contributing to microvascular remodeling and dysfunction [9]. In line with this, we found that the combination of MetS and RVH decreased myocardial capillary density (CD31 staining), which increased in MetS+RVH pigs treated with PTRA. Importantly, endothelial cell mitochondrial density correlated with myocardial capillary density, suggesting that endothelial cell mitochondria protection might be an important mechanism by which PTRA preserves myocardial capillary density. However, PTRA-induced improvements in endothelial cell mitochondria were not accompanied by increments in larger myocardial microvessels, which may take longer to restore. Notably, the resolution of the micro-CT scanner used in this study is unable to capture capillaries and very small arterioles. Yet, myocardial microvascular tortuosity decreased in PTRA-treated pigs, suggesting improved microvascular maturity. In patients with heart failure with preserved ejection fraction, cardiac microvascular function is inversely associated with intracardiac filling pressures [39]. Therefore, our observations have important implications and demonstrate a potential role of PTRA for preserving cardiac microvascular maturity in MetS+RVH.

Myocardial oxidative stress, assessed by in situ production of superoxide anion, increased in MetS+RVH, possibly partly due to increased mitochondrial ROS production. Indeed, myocardial mitochondrial production of H_2O_2 correlated directly with DHE staining. However, MetS+RVH-induced myocardial oxidative stress decreased in pigs treated with PTRA, highlighting the potential of this intervention to modulate myocardial redox status.

Oxidative stress is an important contributor to cardiac structural remodeling and promotes the development of cardiac fibrosis [40]. In agreement, we found that myocyte cross-sectional area, LVMM, and myocardial fibrosis increased in MetS+RVH compared to Sham groups but were attenuated by renal revascularization that also blunted myocardial oxidative stress. Interestingly, we found that interfibrillar and endothelial cell mitochondrial damage correlated with cardiac injury. Thus, preservation of myocardial mitochondria could have been an important mechanism by which PTRA attenuated cardiac injury in experimental MetS+RVH.

Unlike our previous studies in swine models of atherosclerotic and non-atherosclerotic RVH [17–20, 41], PTRA failed to restore blood pressure in MetS+RVH pigs. Possibly, recruitment of additional pressure mechanisms, such as circulating isoprostanes, could have contributed to sustain RVH in these pigs [42]. Systemic isoprostanes are reliable biomarkers of oxidative stress that may directly induce abnormal vascular responses in vivo and in vitro. Indeed, their infusion in hypercholesterolemic pigs is associated with hypertension and oxidative stress [43]. Renal revascularization failed to decrease circulating isoprostane levels, which could have partly accounted to sustain hypertension in PTRA-treated pigs.

Although systolic function remained similar among the groups, PTRA normalized LV relaxation (E/A ratio) and decreased LA EDV, and NT-proBNP levels, suggesting attenuation of diastolic dysfunction. Serum creatinine levels were also restored to normal levels in MetS+RVH+PTRA pigs. Therefore, some of the beneficial effects of PTRA on the heart were likely partly achieved indirectly by the improvement of renal function, in agreement with our previous observations in swine RVH that intra-renal delivery of stem cell-derived extracellular vesicles [44] or chronic administration of mitoprotective drugs [9] preserve cardiac structure and function without altering systemic blood pressure. In line with this, we found that stenotic kidney GFR correlates directly with interfibrillar matrix density and ATP generation, suggesting that improvement of ischemic kidney function by PTRA might contribute to preserve myocardial mitochondria and confer cardioprotection in pigs with coexisting MetS+RVH, independent of its effects on RVH and of continuous MetS.

The mechanisms by which improvement of ischemic kidney function by PTRA could have contribute to preserve cardiac structure and function are multifactorial and may include reductions in renal and systemic inflammation, oxidative stress, fibrotic mediators, uremic toxins, or vasoactive substances. We have shown that both human [45] and pig [20] stenotic kidneys release several inflammatory cytokines to the systemic circulation, and their reduction ameliorates cardiac injury and dysfunction [46]. In line with this, we found that circulating MCP-1 and IL-6 levels decreased in PTRA-treated pigs, suggesting that preservation of renal function by PTRA might have partly contributed to ameliorate cardiac injury and dysfunction by modulating an inflammatory crosstalk between the kidney and the heart. Alternatively, the high beneficial effect of PTRA in the heart could have been secondary to remote ischemic preconditioning effects, in which renal ischemia and subsequent reperfusion might lead to better cardiac outcomes by sending metabolic signals [47]. Although this mechanism could have partly contributed to ameliorate mitochondrial and myocardial oxidative stress, circulating 8-isoprstane levels did not improved in PTRA-treated pigs, arguing against remote ischemic preconditioning effects as a primary mechanism of cardioprotection in our model. Further studies are needed to explore the mechanisms by which PTRA modulates the release of circulating mediators from the ischemic kidney and contributes to preserve the remote myocardial damage in MetS+RVH.

5. Limitations

Our study has some limitations including the short duration of the MetS and RVH, as well as the use of relatively young animals. Yet, our MetS animals developed obesity and hypertension, and our RVH pigs achieved significant stenosis and increased systolic,

diastolic, and mean arterial pressure, which in combination with MetS imparted important changes on the structure and function of the heart. This model cannot discriminate the effects of MetS and RVH on cardiac mitochondria. However, our previous studies in swine demonstrated that diet-induced MetS [7, 8] and surgically induced RVH [9] can independently induce myocardial mitochondrial damage. Furthermore, we found that coexisting MetS and RVH in swine is associated with significant myocardial mitochondrial damage [10]. Although MDCT provides an accurate and detailed evaluation of cardiac structure and function, it has several limitations compared to commonly used imaging modalities such as echocardiography [48]. Although blood pressure was similarly elevated in MetS+Sham and MetS+RVH groups compared to Lean+Sham, PRA levels were similar among the group, as typical to the chronic phase of untreated RVH [49]. Our observations suggest that improvement of renal function by PTRA might confer cardioprotection in MetS+RVH pigs, independent of its effects on blood pressure. Yet, it is important to note that in patients with RVH, PTRA may not improve renal function and may even worsen it [50], limiting the cardioprotective effects of this intervention. Additional studies are needed to assess whether MetS+RVH-induced changes in myocardial mitochondrial structure and function persist for longer periods of time and to validate the clinical efficacy of PTRA in individuals with coexisting MetS and RVH.

6. Conclusions

In summary, our study suggests a novel therapeutic role for renal revascularization in preserving myocardial mitochondrial structure and function in swine MetS+RVH. Importantly, amelioration of cardiac mitochondrial abnormalities and dysfunction was associated with improved myocardial microvascular maturity and attenuation of capillary loss, oxidative stress, and fibrosis, which might have contributed to decrease cardiac remodeling and diastolic dysfunction. Therefore, our observations have important clinical implications by uncovering a novel mechanism by which PTRA improves cardiac outcomes in chronic experimental MetS+RVH. Prospective clinical studies are needed to confirm our findings and define the degree to which myocardial mitochondrial protection by PTRA preserves cardiac structure and function in patients with MetS and RVH.

Supplementary Material

Refer to Web version on PubMed Central for supplementary material.

Funding

This work was supported by the NIH grants: DK122137, DK104273, DK120292, HL095638, DK118120, and DK102325.

Abbreviations

RVH	Renovascular hypertension
MetS	Metabolic syndrome
PTRA	Percutaneous transluminal renal angioplasty

ATP	Adenosine triphosphate
ROS	Reactive oxygen species
LV	Left ventricular
PRA	Plasma renin activity
MCP	Monocyte chemoattractant protein
IL	Interleukin
NT-proBNP	N-terminal pro-brain natriuretic peptide
MDCT	Multi-detector computed tomography
LVMM	LV muscle mass
LA	Left atrium
RBF	Renal blood flow
GFR	Glomerular filtration rate
H_20_2	Hydrogen peroxide
COX-IV	Cytochrome-c oxidase
DHE	Dihydroethidium
WGA	Wheat germ agglutinin
EDV	End-diastolic volume

References

1. Herrmann SM and Textor SC, Renovascular hypertension. Endocrinol Metab Clin North Am, 2019. 48(4): p. 765–778. [PubMed: 31655775]
2. Green D and Kalra PA, The heart in atherosclerotic renovascular disease. Front Biosci (Elite Ed), 2012. 4: p. 856–64. [PubMed: 22201919]
3. Textor SC and Lerman LO, Paradigm shifts in atherosclerotic renovascular disease: Where are we now? J Am Soc Nephrol, 2015. 26(9): p. 2074–80. [PubMed: 25868641]
4. Kane GC, et al. , Renal artery revascularization improves heart failure control in patients with atherosclerotic renal artery stenosis. Nephrol Dial Transplant, 2010. 25(3): p. 813–20. [PubMed: 19666661]
5. Holmuhamedov EL, et al. , Cardiac subsarcolemmal and interfibrillar mitochondria display distinct responsiveness to protection by diazoxide. PLoS One, 2012. 7(9): p. e44667. [PubMed: 22973464]
6. Duchen MR, Mitochondria in health and disease: Perspectives on a new mitochondrial biology. Mol Aspects Med, 2004. 25(4): p. 365–451. [PubMed: 15302203]
7. Yuan F, et al. , Mitochondrial targeted peptides preserve mitochondrial organization and decrease reversible myocardial changes in early swine metabolic syndrome. Cardiovasc Res, 2018. 114(3): p. 431–442. [PubMed: 29267873]
8. Yuan F, et al. , Mitoprotection attenuates myocardial vascular impairment in porcine metabolic syndrome. Am J Physiol Heart Circ Physiol, 2018. 314(3): p. H669–H680. [PubMed: 29196345]

9. Eirin A, et al. , Restoration of mitochondrial cardiolipin attenuates cardiac damage in swine renovascular hypertension. J Am Heart Assoc, 2016. 5(6).
10. Aghajani Nargesi A, et al. , Renovascular hypertension induces myocardial mitochondrial damage, contributing to cardiac injury and dysfunction in pigs with metabolic syndrome. Am J Hypertens, 2020.
11. Eirin A, et al. , Mesenchymal stem cell-derived extracellular vesicles improve the renal microvasculature in metabolic renovascular disease in swine. Cell Transplant, 2018. 27(7): p. 1080–1095. [PubMed: 29954220]
12. Eirin A, et al. , Mesenchymal stem cell-derived extracellular vesicles attenuate kidney inflammation. Kidney Int, 2017. 92(1): p. 114–124. [PubMed: 28242034]
13. Nargesi AA, et al. , Coexisting renal artery stenosis and metabolic syndrome magnifies mitochondrial damage, aggravating poststenotic kidney injury in pigs. J Hypertens, 2019. 37(10): p. 2061–2073. [PubMed: 31465309]
14. Farahani RA, et al. , Percutaneous transluminal renal angioplasty attenuates poststenotic kidney mitochondrial damage in pigs with renal artery stenosis and metabolic syndrome. J Cell Physiol, 2020.
15. Pawar AS, et al. , Adipose tissue remodeling in a novel domestic porcine model of diet-induced obesity. Obesity (Silver Spring), 2015. 23(2): p. 399–407. [PubMed: 25627626]
16. Lerman LO, et al. , Noninvasive evaluation of a novel swine model of renal artery stenosis. J Am Soc Nephrol, 1999. 10(7): p. 1455–65. [PubMed: 10405201]
17. Eirin A, et al. , A mitochondrial permeability transition pore inhibitor improves renal outcomes after revascularization in experimental atherosclerotic renal artery stenosis. Hypertension, 2012. 60(5): p. 1242–9. [PubMed: 23045468]
18. Eirin A, et al. , Persistent kidney dysfunction in swine renal artery stenosis correlates with outer cortical microvascular remodeling. Am J Physiol Renal Physiol, 2011. 300(6): p. F1394–401. [PubMed: 21367913]
19. Eirin A, et al. , Adipose tissue-derived mesenchymal stem cells improve revascularization outcomes to restore renal function in swine atherosclerotic renal artery stenosis. Stem Cells, 2012. 30(5): p. 1030–41. [PubMed: 22290832]
20. Eirin A, et al. , Changes in glomerular filtration rate after renal revascularization correlate with microvascular hemodynamics and inflammation in Swine renal artery stenosis. Circ Cardiovasc Interv, 2012. 5(5): p. 720–8. [PubMed: 23048054]
21. Eirin A, et al. , Persistent kidney dysfunction in swine renal artery stenosis correlates with outer cortical microvascular remodeling. Am J Physiol Renal Physiol, 2011. 300(6): p. F1394–401. [PubMed: 21367913]
22. Eirin A, et al. , Intra-renal delivery of mesenchymal stem cells attenuates myocardial injury after reversal of hypertension in porcine renovascular disease. Stem Cell Res Ther, 2015. 6: p. 7. [PubMed: 25599803]
23. Rodriguez-Porcel M, et al. , Long-term antioxidant intervention improves myocardial microvascular function in experimental hypertension. Hypertension, 2004. 43(2): p. 493–8. [PubMed: 14718362]
24. Zhu XY, et al. , Simvastatin prevents coronary microvascular remodeling in renovascular hypertensive pigs. J Am Soc Nephrol, 2007. 18(4): p. 1209–17. [PubMed: 17344424]
25. Krier JD, et al. , Noninvasive measurement of concurrent single-kidney perfusion, glomerular filtration, and tubular function. Am J Physiol Renal Physiol, 2001. 281(4): p. F630–8. [PubMed: 11553509]
26. Eirin A, et al. , Urinary mitochondrial DNA copy number identifies chronic renal injury in hypertensive patients. Hypertension, 2016. 68(2): p. 401–10. [PubMed: 27324229]
27. Krier JD, et al. , Noninvasive measurement of concurrent single-kidney perfusion, glomerular filtration, and tubular function. Am J Physiol Renal Physiol, 2001. 281(4): p. F630–8. [PubMed: 11553509]
28. Pi J, et al. , Reactive oxygen species as a signal in glucose-stimulated insulin secretion. Diabetes, 2007. 56(7): p. 1783–91. [PubMed: 17400930]

29. Eirin A, et al. , Mitochondrial targeted peptides attenuate residual myocardial damage after reversal of experimental renovascular hypertension. J Hypertens, 2014. 32(1): p. 154–65. [PubMed: 24048008]
30. Conlon PJ, et al. , Severity of renal vascular disease predicts mortality in patients undergoing coronary angiography. Kidney Int, 2001. 60(4): p. 1490–7. [PubMed: 11576364]
31. Wright JR, et al. , Left ventricular morphology and function in patients with atherosclerotic renovascular disease. J Am Soc Nephrol, 2005. 16(9): p. 2746–53. [PubMed: 16049071]
32. Cooper CJ, et al. , Stenting and medical therapy for atherosclerotic renal-artery stenosis. N Engl J Med, 2014. 370(1): p. 13–22. [PubMed: 24245566]
33. Ritchie J, et al. , High-risk clinical presentations in atherosclerotic renovascular disease: Prognosis and response to renal artery revascularization. Am J Kidney Dis, 2014. 63(2): p. 186–97. [PubMed: 24074824]
34. Hollander JM, Thapa D, and Shepherd DL, Physiological and structural differences in spatially distinct subpopulations of cardiac mitochondria: influence of cardiac pathologies. Am J Physiol Heart Circ Physiol, 2014. 307(1): p. H1–14. [PubMed: 24778166]
35. Wong HS, et al. , Production of superoxide and hydrogen peroxide from specific mitochondrial sites under different bioenergetic conditions. J Biol Chem, 2017. 292(41): p. 16804–16809. [PubMed: 28842493]
36. Li Y, et al. , Cytochrome c oxidase subunit IV is essential for assembly and respiratory function of the enzyme complex. J Bioenerg Biomembr, 2006. 38(5-6): p. 283–91. [PubMed: 17091399]
37. Bao L, et al. , Mitochondria are the source of hydrogen peroxide for dynamic brain-cell signaling. J Neurosci, 2009. 29(28): p. 9002–10. [PubMed: 19605638]
38. Kluge MA, Fetterman JL, and Vita JA, Mitochondria and endothelial function. Circ Res, 2013. 112(8): p. 1171–88. [PubMed: 23580773]
39. Ahmad A, et al. , Coronary microvascular dysfunction is associated with exertional haemodynamic abnormalities in patients with heart failure with preserved ejection fraction. Eur J Heart Fail, 2020.
40. Zhao W, et al. , Oxidative stress mediates cardiac fibrosis by enhancing transforming growth factor-beta1 in hypertensive rats. Mol Cell Biochem, 2008. 317(1-2): p. 43–50. [PubMed: 18581202]
41. Eirin A, et al. , Endothelial outgrowth cells shift macrophage phenotype and improve kidney viability in swine renal artery stenosis. Arterioscler Thromb Vasc Biol, 2013. 33(5): p. 1006–13. [PubMed: 23430615]
42. Lerman LO, et al. , Increased oxidative stress in experimental renovascular hypertension. Hypertension, 2001. 37(2 Pt 2): p. 541–6. [PubMed: 11230332]
43. Wilson SH, et al. , Enhanced coronary vasoconstriction to oxidative stress product, 8-epi-prostaglandinF2 alpha, in experimental hypercholesterolemia. Cardiovasc Res, 1999. 44(3): p. 601–7. [PubMed: 10690293]
44. Zhang L, et al. , Selective intrarenal delivery of mesenchymal stem cell-derived extracellular vesicles attenuates myocardial injury in experimental metabolic renovascular disease. Basic Res Cardiol, 2020. 115(2): p. 16. [PubMed: 31938859]
45. Eirin A, et al. , Inflammatory and injury signals released from the post-stenotic human kidney. Eur Heart J, 2013. 34(7): p. 540–548a. [PubMed: 22771675]
46. Urbieta-Caceres VH, et al. , Selective improvement in renal function preserved remote myocardial microvascular integrity and architecture in experimental renovascular disease. Atherosclerosis, 2012. 221(2): p. 350–8. [PubMed: 22341593]
47. Tapuria N, et al. , Remote ischemic preconditioning: A novel protective method from ischemia reperfusion injury--a review. J Surg Res, 2008. 150(2): p. 304–30. [PubMed: 19040966]
48. Mangalat D, et al. , Value of cardiac CT in patients with heart failure. Curr Cardiovasc Imaging Rep, 2009. 2(6): p. 410–417. [PubMed: 20369033]
49. Pipinos II, et al. , Response to angiotensin inhibition in rats with sustained renovascular hypertension correlates with response to removing renal artery stenosis. J Vasc Surg, 1998. 28(1): p. 167–77. [PubMed: 9685143]
50. Safian RD and Madder RD, Refining the approach to renal artery revascularization. JACC Cardiovasc Interv, 2009. 2(3): p. 161–74. [PubMed: 19463421]

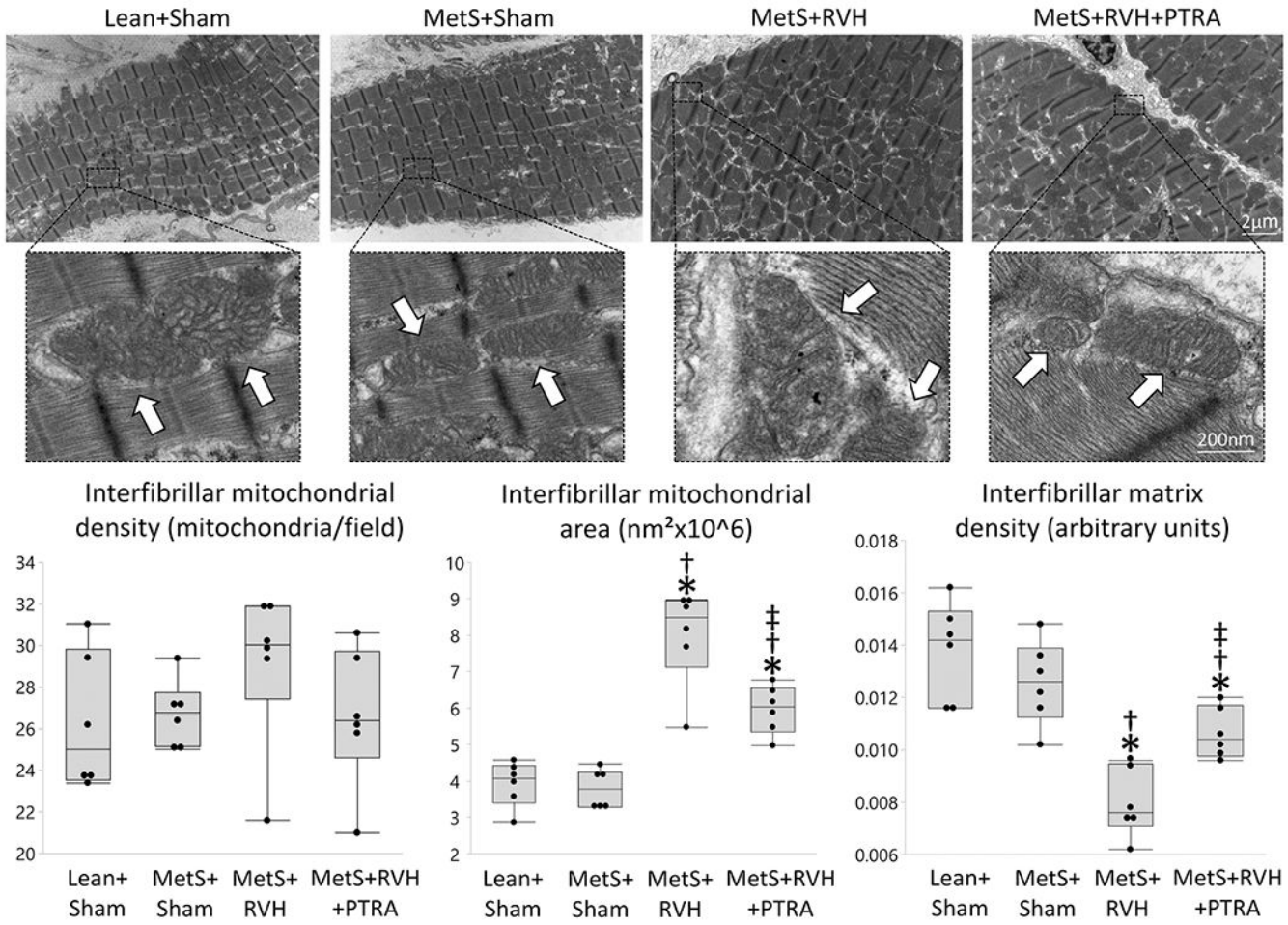

Figure 1.

PTRA attenuated myocardial mitochondrial structural damage. Representative transmission electron microscopy images of interfibrillar mitochondria (arrows) and quantification of mitochondrial density, area, and matrix density in study groups (n=6/group each). *p<0.05 vs. Lean+Sham; †p<0.05 vs. MetS+Sham; ‡p<0.05 vs. MetS+RVH.

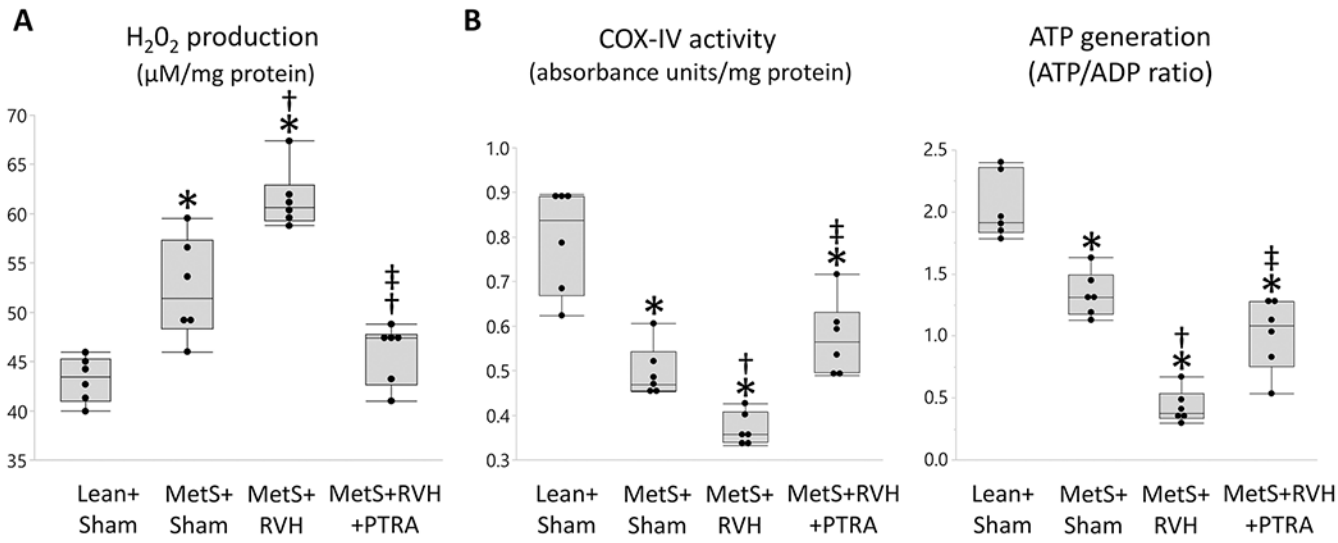

Figure 2.

Renal revascularization improved cardiac mitochondrial function. Quantification of myocardial mitochondrial hydrogen peroxide (H_20_2) production (**A**), cytochrome-c oxidase (COX)-IV activity (**B**), and ATP/ADP ratio (**C**) in study groups (n=6/group each). *p<0.05 vs. Lean+Sham; †p<0.05 vs. MetS+Sham; ‡p<0.05 vs. MetS+RVH.

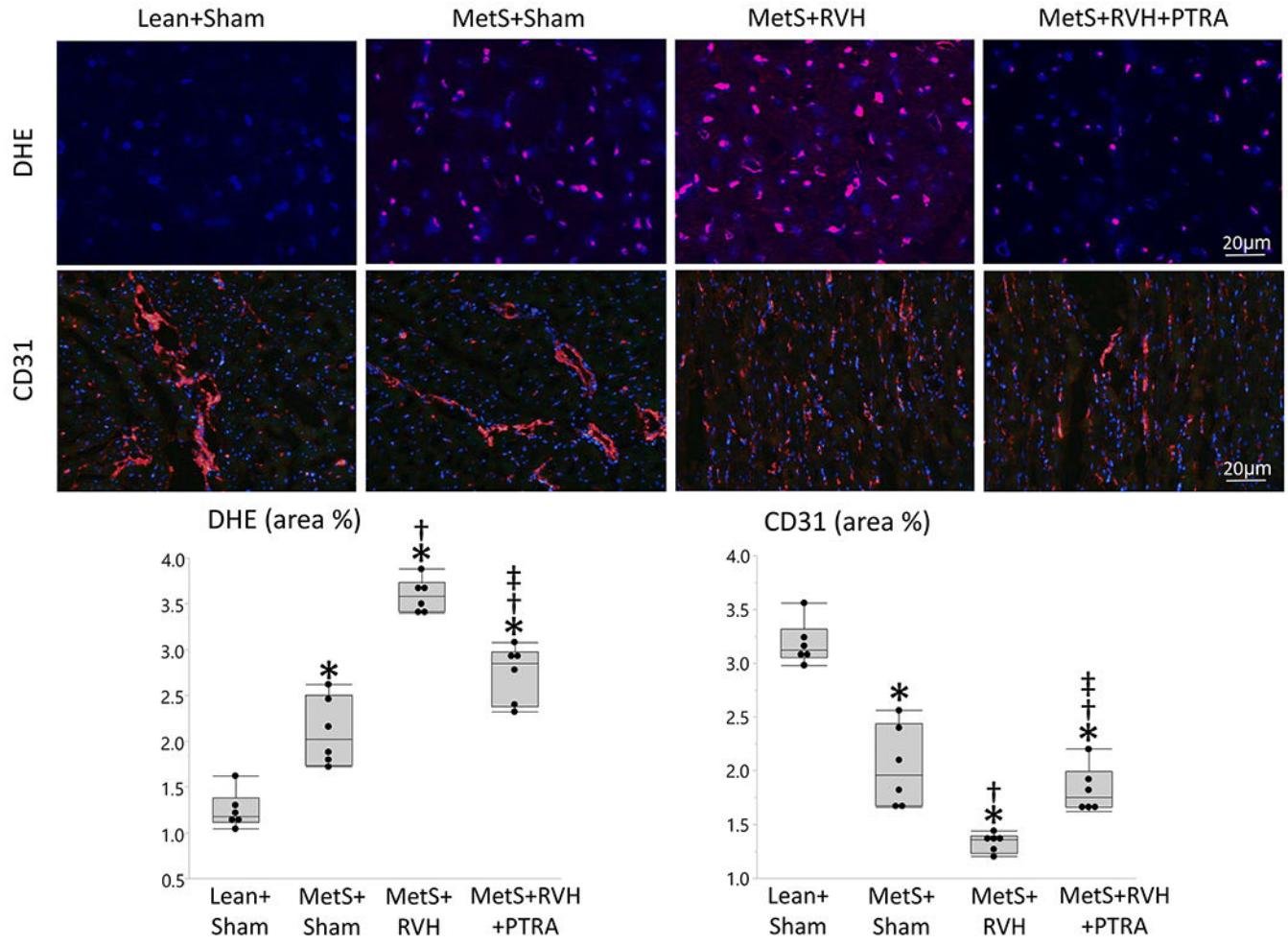

Figure 3.

PTRA attenuated cardiac oxidative stress and improved capillary density. Representative myocardial dihydroethidium (DHE, red) and immunofluorescence staining of CD31, and quantification of myocardial production of superoxide anion (DHE area %) and myocardial capillary density (CD31 area %) (n=6/group each). *p<0.05 vs. Lean+Sham; †p<0.05 vs. MetS+Sham; ‡p<0.05 vs. MetS+RVH.

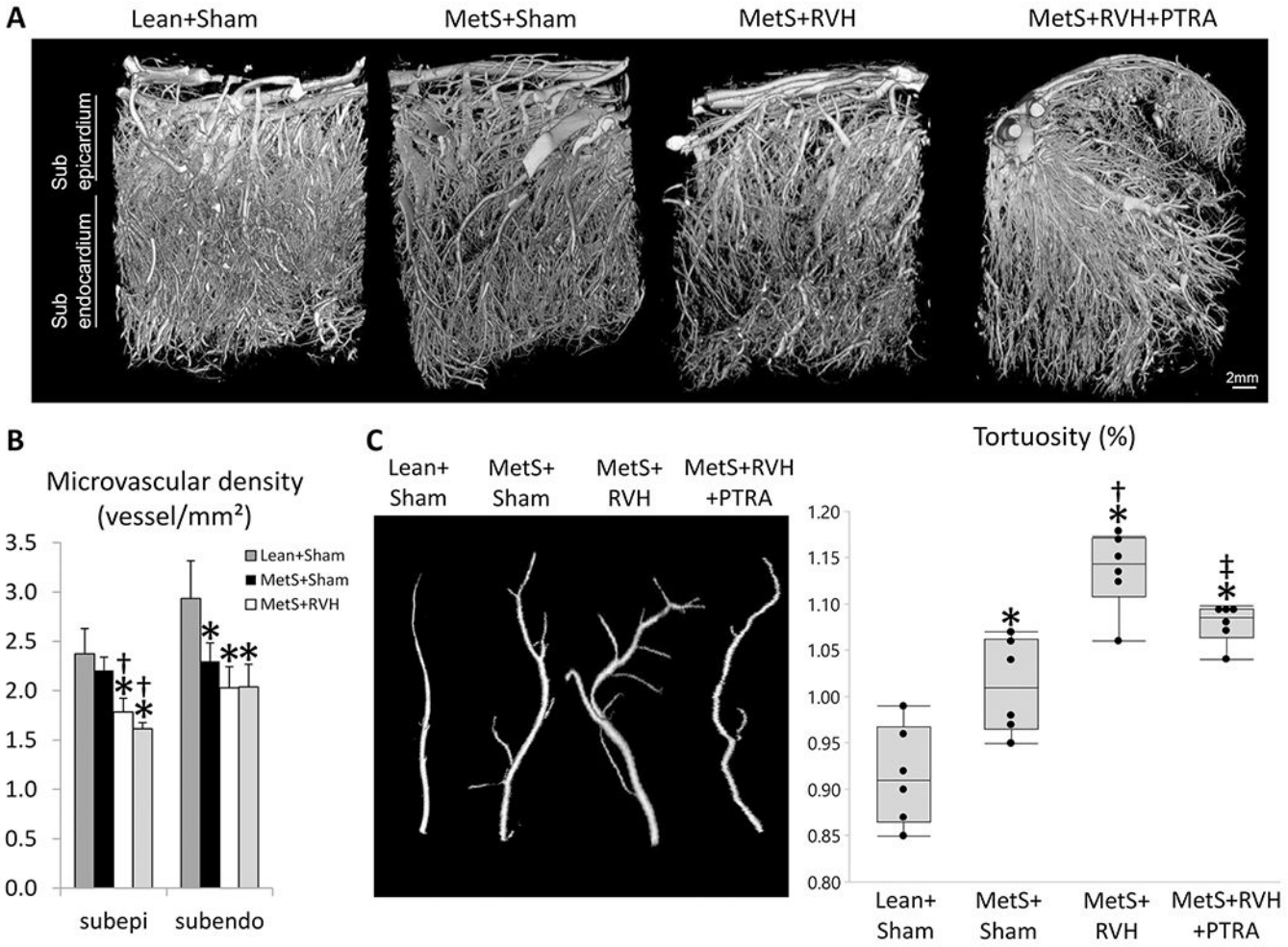

Figure 4.

Renal revascularization improved myocardial microvascular maturity. **A** Representative 3D micro-computed tomography images of the left ventricle in study groups. **B** Quantification of spatial density of microvessels in the subepicardium and subendocardium. **C** Quantification of microvascular tortuosity in study groups. *p<0.05 vs. Lean+Sham; †p<0.05 vs. MetS+Sham; ‡p<0.05 vs. MetS+RVH.

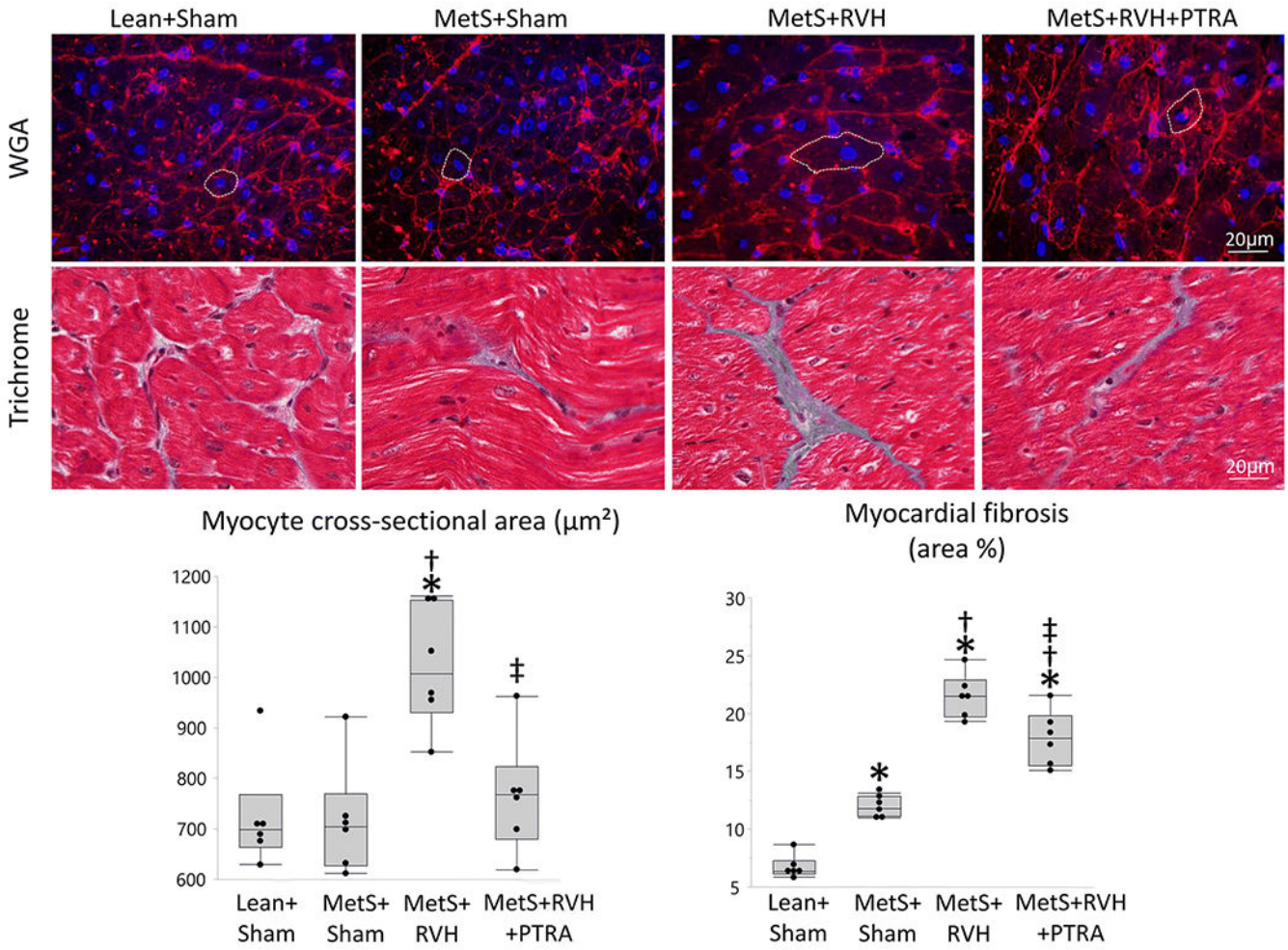

Figure 5.

Renal revascularization ameliorated LV remodeling and fibrosis. Representative LV sections stained with wheat germ agglutinin (WGA) and trichrome, and quantification of myocyte cross-sectional area and myocardial fibrosis in Lean+Sham, MetS+Sham, MetS+RVH, and MetS+RVH+PTRA. *p<0.05 v Lean+Sham; †p<0.05 vs. MetS+Sham; ‡p<0.05 vs. MetS+RVH.

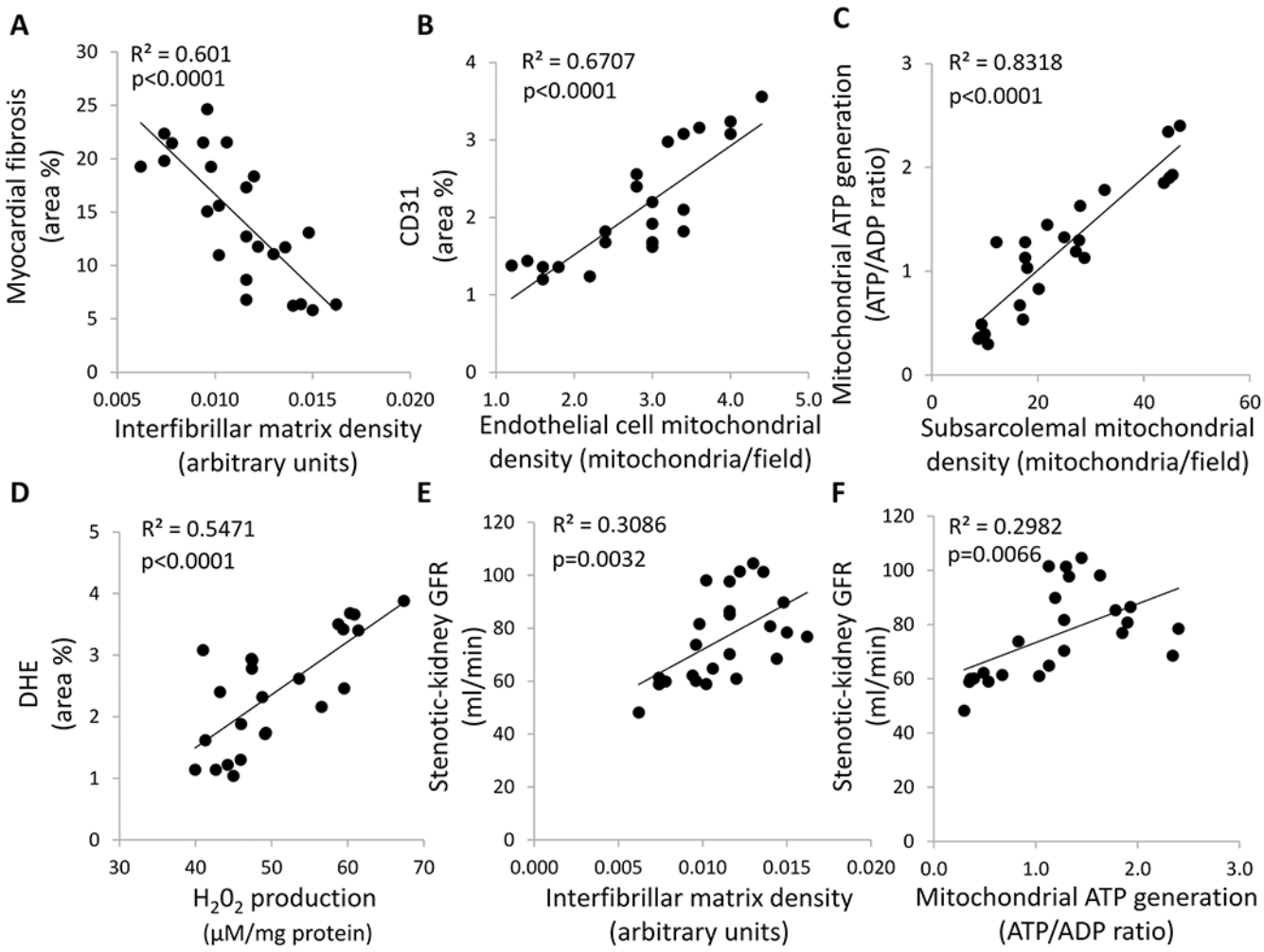

Figure 6.

Cardiac mitochondrial damage correlated with myocardial injury. **A** Myocardial mitochondrial matrix density correlated inversely with myocardial fibrosis. **B** Endothelial cell mitochondrial density correlated directly with myocardial capillary density (CD31 area %). **C** Subsarcolemmal mitochondrial density correlated directly with cardiac mitochondrial ATP generation. **D** Myocardial mitochondrial H_20_2 production ATP generation correlated directly with myocardial production of superoxide anion (DHE area %). **E** Myocardial mitochondrial matrix density correlated directly with stenotic kidney GFR. **F** Myocardial mitochondrial ATP generation correlated directly with stenotic kidney GFR.

Table 1.

Systemic characteristics and cardiac function in study groups at 16 weeks (n=6 each).

	Lean+Sham	MetS+Sham	MetS+RVH	MetS+RVH+PTRA
Body weight (kg)	71.1 ± 1.8	93.9 ± 1.0 *	90.9 ± 2.8 *	90.9 ± 3.3 *
Heart rate (bpm)	82.3 ± 7.1	75.2 ± 5.7	86.3 ± 6.2	82.1 ± 7.3
SBP (mmHg)	129.8 ± 4.2	148.8 ± 4.1 *	167.1 ± 8.0 *	166.1 ± 8.5 *
DBP (mmHg)	92.2 ± 2.7	112.8 ± 4.4 *	120.8 ± 6.7 *	111.1 ± 3.5 *
MAP (mmHg)	104.7 ± 2.0	124.8 ± 4.3 *	136.2 ± 7.1 *	129.4 ± 3.4 *
Degree of stenosis (%)	0.0 ± 0.0	0.0 ± 0.0	86.3 ± 4.7 *†	0.0 ± 0.0‡
PRA (ng/ml/h)	0.13 ± 0.09	0.15 ± 0.06	0.15 ± 0.13	0.14 ± 0.15
MCP-1 (pg/ml)	120.9 ± 46.7	135.9 ± 46.3	262.1 ± 68.1 *†	178.3 ± 37.6 *†‡
IL-6 (pg/ml)	2.7 ± 2.1	3.6 ± 2.4	85.0 ± 53.3 *†	19.2 ± 18.4 *†‡
8-Isoprostane (pg/ml)	87.5 ± 10.0	138.9 ± 37.5 *	321.5 ± 97.3 *†	338.5 ± 119.5 *†
Serum creatinine (mg/dl)	1.22 ± 0.01	1.27 ± 0.05	1.93 ± 0.02 *†	1.62 ± 0.13 *†‡
Renal volume (ml)	142.9 ± 4.2	188.2 ± 4.1 *	151.4 ± 1.3 *†	169.3 ± 9.1 *†‡
RBF (ml/min)	649.2 ± 31.4	831.3 ± 36.2 *	549.0 ± 23.8 *†	649.2 ± 29.3 †‡
GFR (ml/min)	79.4 ± 2.7	98.8 ± 2.1 *	58.4 ± 2.1 *†	68.4 ± 3.5 *†‡
LA EDV (ml)	55.5 ± 4.9	64.0 ± 4.5	75.1 ± 7.1 *	65.8 ± 8.7
LVMM (g)	123.8 ± 7.3	127.4 ± 4.5	177.2 ± 3.5 *†	153.2 ± 10.3 *†‡
Ejection fraction (%)	50.8 ± 2.4	49.1 ± 1.5	54.7 ± 2.3	53.2 ± 1.3
E/A ratio	1.3 ± 0.1	1.3 ± 0.1	0.7 ± 0.1 *†	1.2 ± 0.1‡
NT-proBNP (pg/ml)	19.5 ± 4.7	33.0 ± 6.4	94.1 ± 12.1 *†	54.4 ± 9.3 *‡

MetS metabolic syndrome, *RVH* renovascular hypertension, *SBP* systolic blood pressure, *DBP* diastolic blood pressure, *MAP* mean arterial pressure, *PRA* plasma renin activity, *MCP* monocyte chemoattractant protein, *IL* interleukin, *RBF* renal blood flow, *GFR* glomerular filtration rate, *LA* left atrium, *EDV* end-diastolic volume, *LVMM* left ventricular muscle mass, *E/A* early (E) and late (A) ventricular filling, *NT-proBNP* N-terminal pro-brain natriuretic peptide

* p<0.05 vs. Lean+Sham

† p<0.05 vs. MetS+Sham

‡ p<0.05 vs. MetS+RVH